Two-component heterogeneous nucleation kinetics and an application to Mars

Anni Määttänen,[a] Hanna Vehkamäki, Antti Lauri, Ismo Napari, and Markku Kulmala
Division of Atmospheric Sciences, Department of Physical Sciences, University of Helsinki, 00014 Helsinki, Finland

(Received 19 December 2006; accepted 19 July 2007; published online 4 October 2007)

We develop a two-component heterogeneous nucleation model that includes exact calculation of the Stauffer-type [D. Stauffer, J. Aerosol Sci. **7**, 319 (1976)] steady-state kinetic prefactor using the correct heterogeneous Zeldovich factor for a heterogeneous two-component system. The model, and a simplified version of it, is tested by comparing its predictions to experimental data for water-*n*-propanol nucleating on silver particles. The model is then applied to water-carbon dioxide system in Martian conditions, which has not been modeled before. Using the ideal mixture assumption, the model shows theoretical possibilities for two-component nucleation adjacent to the initial stages of one-component water nucleation, especially with small water vapor amounts. The numbers of carbon dioxide molecules in the critical cluster are small in the case of large water amounts (up to 300 ppm) in the gas phase, but larger when there is very little water vapor (1 ppm). © *2007 American Institute of Physics*. [DOI: 10.1063/1.2770737]

I. INTRODUCTION

Clouds have been known to exist on Mars since the beginning of observations of the Martian atmosphere and they exhibit clear temporal and spatial patterns. Water ice clouds have been directly identified from observations and CO_2 clouds were observed indirectly.[1–4] In certain situations, for example, in the polar night, the atmosphere is depleted of water, and in the cold polar winter temperatures, CO_2 clouds are formed. CO_2 clouds also form at very high altitudes in the equatorial areas, as observed recently by SPICAM and OMEGA on Mars Express.[5–7] In some areas the temperatures are too high for CO_2 condensation, but low enough for the water vapor in the atmosphere to nucleate and condense. Thus the previous studies on modeling the formation of Martian clouds have focused mostly on describing one type of clouds at a time.[8–16] It has been shown through a thermodynamic analysis of the system of these major Martian volatiles ($CO_2$and H_2O)[17] that the two components together can theoretically condense as a clathrate or an eutectic mixture of CO_2 ice with clathrate or H_2O ice. Also Ref. 18 studied the formation and remote sensing detectability of CO_2 clathrate hydrate in Martian conditions. These studies raise the question of possible formation of ice particles composed of H_2O and CO_2 in the atmosphere. The goal of this paper is to study this phenomenon of two-component nucleation in the atmosphere of Mars in a theoretical framework.

We tested different approaches of nucleation kinetics as a prelude for the main interest of our work: the Martian CO_2-H_2O system. This paper also presents the first model study of two-component heterogeneous nucleation using the exact Stauffer steady-state kinetics,[19,20] which we refer to as Stauffer kinetics from now on. Several approximations have been used previously in the literature and we wanted to avoid using them before testing their effect. We have compared the Stauffer kinetics and the approximate models to each other, and to experimental data using water-*n*-propanol system, which served as a test bench for the models. The structure of the paper is as follows: In Sec. II we focus on the classical theory of nucleation, first presenting the basics of the well-understood thermodynamics, after which we focus on the kinetics, both the exact Stauffer kinetics and the different approximations commonly used. We also discuss briefly the presentation of results in terms of nucleation probability, a key concept in heterogeneous nucleation. In Sec. III we present the comparison of the different kinetic approaches and compare the results to experimental data. This section forms the foundation for the model selection. Finally, in Sec. IV we focus on the main point of this paper, which is modeling the nucleation of the Martian CO_2-H_2O system. We discuss the approximations made, a correction for nonisothermal nucleation that has been previously used in the literature but which is unnecessary in general in heterogeneous nucleation, and the difficulties involved with the exotic CO_2-H_2O system. This section presents the first ever testing of two-component particle formation in the Martian atmosphere. In Sec. V we summarize and discuss the results of the comparison of the kinetic approaches and modeling of the Martian system. The appendices describe more in detail the calculation of the formation free energy for a general cluster and summarize some of the thermodynamic data for the two systems used in this work.

II. THE HETEROGENEOUS TWO-COMPONENT NUCLEATION THEORY

A. Thermodynamics and critical cluster composition

In heterogeneous nucleation clusters form on the surfaces of pre-existing solid condensation nuclei (CN). To dis-

[a]Also at Space Research, Finnish Meteorological Institute. Electronic mail: anni.maattanen@helsinki.fi

 © 2007 American Institute of Physics

Downloaded 19 Dec 2007 to 128.214.182.209. Redistribution subject to AIP license or copyright; see http://jcp.aip.org/jcp/copyright.jsp

tinguish the cluster from the CN we call the cluster phase liquid, but this is only a matter of terminology: clusters can be either liquid or solid, and in fact the phase of a small cluster consisting of only a few molecules is not necessarily well defined.

In the two-component heterogeneous case the mole fraction x (of for example component 2) in the liquid core of the critical cluster is obtained as in the homogeneous case[21] by solving the equation

$$\frac{\Delta\mu_1(x)}{v_1(x)} = \frac{\Delta\mu_2(x)}{v_2(x)} \tag{1}$$

and the radius is given by the Kelvin equation

$$r^* = \frac{2\sigma_{g,l}v_i}{\Delta\mu_i}, \tag{2}$$

where subscripts 1 and 2 refer to the two substances and subscript i to either of them. The formation free energy of the homogeneous critical cluster is

$$\Delta G^*_{\text{hom}} = \frac{4}{3}\pi r^{*2}\sigma_{g,l}. \tag{3}$$

In these equations $\sigma_{g,l}$ is the gas-liquid surface tension, v_i the partial molecular volume in the liquid of component i, and r^* is the radius of the critical cluster. For ideal gas the chemical potential difference [the difference between the chemical potential of the vapor $\mu_{i,g}(P_g,x_{i,g})$ and the chemical potential of the liquid at the vapor pressure $\mu_{i,l}(P_g,x_{i,l})$] is $\Delta\mu_i=-kT\ln[A_{i,g}/A_{i,l}(x)]$, where $A_{i,g}$ and $A_{i,l}$ are the gas and liquid phase activities, respectively.

The formation energy for a heterogeneous cluster can be expressed with the help of the formation energy of a homogeneous cluster at the same gas phase conditions as[22]

$$\Delta G_{\text{het}} = f_g \Delta G_{\text{hom}}, \tag{4}$$

where f_g is a geometric factor. The number of molecules in the heterogeneous critical cluster is connected to the number of molecules in the homogeneous cluster through another geometric factor, $f_n=\Delta N_{\text{het}}/\Delta N_{\text{hom}}$, which can be acquired from the ratio of volumes $V_{\text{het}}/V_{\text{hom}}$ assuming the same bulk liquid density for heterogeneous and homogeneous clusters.

The geometric factors depend on the shape of both the nucleating cluster and the pre-existing particle. For a cluster which is part of a sphere (see Fig. 1) and a spherical pre-existing particle the factor f_g is given by[22]

$$f_g = \frac{1}{2}\left\{1+\left(\frac{1-Xm}{g}\right)^3 + X^3\left[2-3\left(\frac{X-m}{g}\right) + \left(\frac{X-m}{g}\right)^3\right] + 3X^3 m\left(\frac{X-m}{g}-1\right)\right\}, \tag{5}$$

where $g=\sqrt{1+X^2-2Xm}$, $X=R_{\text{CN}}/r^*$, R_{CN} is the radius of the pre-existing particle, and r^* the radius of the critical cluster. The contact parameter $m=\cos\theta$ is given by Young's equation as

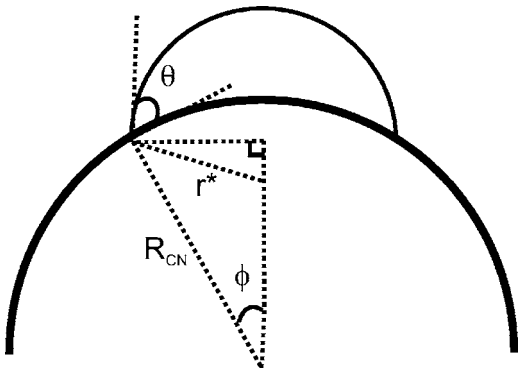

FIG. 1. The geometry of heterogeneous nucleation: a critical cluster of radius r^* on the surface of a pre-existing particle of radius R_{CN}. θ is the contact angle. Angle ϕ is related to Eqs. (24) and (25).

$$m(x) = \cos\theta = \frac{\sigma_{g,\text{sol}} - \sigma_{l,\text{sol}}(x)}{\sigma_{g,l}(x)}, \tag{6}$$

where θ is the contact angle between the liquid and the pre-existing particle (see Fig. 1), $\sigma_{g,\text{sol}}$ is the surface tension between the gas and solid phases, and $\sigma_{l,\text{sol}}$ is the surface tension between the liquid and solid phases. For the geometry of Fig. 1 the geometric factor f_n reads[22,23]

$$f_n = \frac{1}{4}\left\{2+3\left(\frac{1-Xm}{g}\right)-\left(\frac{1-Xm}{g}\right)^3 - X^3\left[2-3\left(\frac{X-m}{g}\right)+\left(\frac{X-m}{g}\right)^3\right]\right\}. \tag{7}$$

For a planar pre-existing surface $X\to\infty$ and the two geometric factors are equal, $f_g=f_n$, but for a spherical condensation nucleus $f_g\neq f_n$.

The bulk molecular numbers in the cluster core are given by

$$n^{\text{het}}_{i,l} = x_i V_{\text{het}}\rho_l(x), \tag{8}$$

where $\rho_l(x)$ is the molecular number density in the bulk liquid and x_i is the mole fraction of component i. The homogeneous cluster volume is $V_{\text{hom}}=\frac{4}{3}\pi r^{*3}$ and the heterogeneous cluster volume is thus $V_{\text{het}}=f_n\cdot\frac{4}{3}\pi r^{*3}$. The total number of molecules in the heterogeneous cluster can be calculated as $n^{\text{het}}_{i,\text{tot}}=n^{\text{het}}_{i,l}+\Sigma_s n^{\text{het}}_{i,s}$ for both substances ($i=1,2$), where $n^{\text{het}}_{i,s}$ is the surface excess number for component i related to interface s. Both gas-liquid $s=(g,l)$ and liquid-solid $s=(l,\text{sol})$ interfaces contribute to the surface excess numbers. The surface excess molecule correction terms can be acquired from[24]

$$n^{\text{het}}_{1,s} = \frac{A_{s,\text{het}}\frac{\partial\sigma_s}{\partial x}}{\frac{v_1}{v_2}\left(\frac{\partial\mu_{2,l}}{\partial x}\right)_r - \left(\frac{\partial\mu_{1,l}}{\partial x}\right)_r},$$
$$n^{\text{het}}_{2,s} = \frac{A_{s,\text{het}}\frac{\partial\sigma_s}{\partial x}}{\frac{v_2}{v_1}\left(\frac{\partial\mu_{1,l}}{\partial x}\right)_r - \left(\frac{\partial\mu_{2,l}}{\partial x}\right)_r}, \tag{9}$$

where $A_{s,\text{het}}$ is the surface area of the interface s, which for gas-liquid surface can be calculated as[22]

Downloaded 19 Dec 2007 to 128.214.182.209. Redistribution subject to AIP license or copyright; see http://jcp.aip.org/jcp/copyright.jsp

$$A_{g,l,\mathrm{het}} = 2\pi r^{*2}\left[1 + \frac{(1 - Xm)}{g}\right] \tag{10}$$

and for liquid-solid surface as

$$A_{l,\mathrm{sol,het}} = 2\pi R_{\mathrm{CN}}^2\left[1 + \frac{(X - m)}{g}\right]. \tag{11}$$

The liquid chemical potentials $\mu_{i,l}$ and their derivatives with respect to mole fraction x are calculated as in Noppel *et al.*[24] The derivative of the liquid-solid surface tension $\sigma_{l,\mathrm{sol}}$ with respect to mole fraction x in the liquid is calculated using Young's equation [Eq. (6)] assuming that the gas-solid surface tension $\sigma_{g,\mathrm{sol}}$ is independent of the liquid composition.

B. Kinetics of nucleation

For the kinetic prefactor in the heterogeneous case the birth-death equations governing the cluster concentrations can be formulated in an analogous way to the homogeneous case. The only difference is that the coefficients giving the collision rate of monomers to the cluster now describe either direct vapor deposition or surface diffusion to the cluster (see later). Assuming steady-state conditions, the birth-death equations together with an equation for the evaporation coefficients (again mathematically equivalent to the homogeneous case) lead to a heterogeneous form of the Stauffer formula (see Ref. 25 for detailed derivation of this equation in the homogeneous case).

Giving the nucleation rate per unit time and unit area of pre-existing surface, the heterogeneous Stauffer formula in the two-component case is[19,20]

$$J = R_{\mathrm{av}} F^e \exp\left(\frac{-\Delta G_{\mathrm{het}}^*}{kT}\right) Z, \tag{12}$$

which has units $\mathrm{m}^{-2}\,\mathrm{s}^{-1}$, where T is the temperature and k is the Boltzmann constant. The factor F^e in the equation of nucleation rate [Eq. (12)] can be approximated as the total number of adsorbed molecules per unit surface area of CN,

$$F^e \approx (c_{1,s}^{\mathrm{ads}} + c_{2,s}^{\mathrm{ads}}). \tag{13}$$

The average growth rate R_{av} is defined as

$$R_{\mathrm{av}} = \frac{\beta_1\beta_2}{\beta_1 \sin^2 \Upsilon + \beta_2 \cos^2 \Upsilon}, \tag{14}$$

where β_i describes the rate of collisions of monomers of species i onto the cluster (here only monomer-cluster interactions are taken into account). The direction angle Υ of the growth vector in size space in the accurate and approximate cases can be expressed as

$$\Upsilon = \arctan\left[\frac{-W_{11}^*\beta_1^* + W_{22}^*\beta_2^*}{2W_{12}^*\beta_1^*} - \frac{\sqrt{4W_{12}^*\beta_1^*W_{12}^*\beta_2^* + (W_{11}^*\beta_1^* - W_{22}^*\beta_2^*)^2}}{2W_{12}^*\beta_1^*}\right] = \Upsilon_{\mathrm{acc.}}, \tag{15}$$

$$\Upsilon = \arctan\frac{x}{1-x} = \Upsilon_{\mathrm{approx.}}. \tag{16}$$

In the latter form the direction angle is assumed to be given by the location of the critical cluster in particle number space.

The matrix W^* is formed from the second derivatives of the formation free energy

$$W^* = \begin{bmatrix} \left(\frac{\partial^2 \Delta G_{\mathrm{het}}}{\partial n_1^2}\right)^* & \left(\frac{\partial^2 \Delta G_{\mathrm{het}}}{\partial n_1\,\partial n_2}\right)^* \\ \left(\frac{\partial^2 \Delta G_{\mathrm{het}}}{\partial n_1\,\partial n_2}\right)^* & \left(\frac{\partial^2 \Delta G_{\mathrm{het}}}{\partial n_2^2}\right)^* \end{bmatrix} \equiv \begin{pmatrix} W_{11}^* & W_{12}^* \\ W_{12}^* & W_{22}^* \end{pmatrix}, \tag{17}$$

where the derivatives are performed with respect to the total numbers in the heterogeneous cluster $n_i = n_{i,\mathrm{tot}}^{\mathrm{het}}$.

The Zeldovich factor Z appearing in the nucleation rate (12) can be calculated in three ways

$$Z = \frac{-(W_{11}^* + 2W_{12}^* \tan \Upsilon + W_{22}^* \tan \Upsilon)}{1 + \tan \Upsilon} \frac{1}{\sqrt{|\det W^*|}} = Z_{\mathrm{acc.}}, \tag{18}$$

$$Z = \sqrt{\frac{\sigma}{kT}} \frac{v_m}{2\pi r^{*2}} = Z_{\mathrm{approx.}}, \tag{19}$$

$$Z = 1, \tag{20}$$

where Eq. (20) is the simplest case of Z being set to unity. Equation (18) is the accurate Stauffer formula and Eq. (19) is the approximate case where the one-component homogeneous expression is extended to the two-component case using the virtual monomer volume v_m (the "average" molecule colliding with the surface of the cluster)

$$v_m = xv_1 + (1 - x)v_2, \tag{21}$$

where v_i are the bulk liquid partial molecular volumes of the species.

Two commonly used classical approaches exist for describing the growth rate of the embryo. The direct vapor deposition approach takes into account only the vapor monomers colliding directly with the critical cluster [Eq. (22)], whereas the surface diffusion approach considers only the monomers that have collided and adhered to the surface of the CN, after which they diffuse to the cluster [Eq. (23)],

$$\beta_i = A_{g,l,\mathrm{het}} \frac{p_{i,g}}{\sqrt{2\pi kTm_i}}, \tag{22}$$

$$\beta_i = 2\pi R_{\mathrm{CN}} \sin\phi d_i c_{i,s}^{\mathrm{ads}} \nu_i \exp\left(\frac{-\Delta F_{i,\mathrm{sd}}}{kT}\right). \tag{23}$$

Here d_i is the mean jump distance of a molecule, $p_{i,g}$ is the pressure in the nucleating vapor, m_i is the mass of a molecule, ν_i is the vibration frequency of a molecule on the surface, and $\Delta F_{i,\mathrm{sd}}$ is the surface diffusion energy. The circumference of the cap

Downloaded 19 Dec 2007 to 128.214.182.209. Redistribution subject to AIP license or copyright; see http://jcp.aip.org/jcp/copyright.jsp

TABLE I. Choices for describing the heterogeneous kinetics in nucleation. $Z_{acc.}$ is the accurate Zeldovich factor described by Eq. (18) and $Z_{approx.}$ the approximate Zeldovich factor described by Eqs. (19) and (21). The growth models direct vapor deposition (DVD) and surface diffusion (SD) are described by Eqs. (22) and (23), respectively.

β / Z	DVD	SD
$Z_{acc.}$ [Eq. (18)] $+\Upsilon_{acc.}$	$Z_{acc.}$+DVD	$Z_{acc.}$+SD
$Z_{approx.}$ [Eq. (19)] $+\Upsilon_{approx.}$	$Z_{approx.}$+DVD	$Z_{approx.}$+SD
$Z=1$ [Eq. (20)] $+\Upsilon_{approx.}$	$Z=1$+DVD	$Z=1$+SD

$$s = 2\pi R_{CN} \sin \phi \tag{24}$$

is calculated here for a spherical CN (Ref. 22) with the angle ϕ given by

$$\cos \phi = (X - m)/g. \tag{25}$$

In expressions (13) and (23) the surface concentrations of monomers, $c_{i,s}^{ads}$, are calculated using a steady state between incoming and outgoing molecule fluxes[26]

$$c_{i,s}^{ads} = \frac{p_{i,g}}{\nu_i \sqrt{2\pi kTm_i}} \exp\left(\frac{\Delta F_{i,des}}{kT}\right), \tag{26}$$

where $\Delta F_{i,des}$ is the desorption energy for component i.

The different choices for the kinetic model in nucleation are described in Table I. As Table I shows, the accurate direction angle Υ is used always when the accurate Zeldovich factor is used, but when using the approximate Zeldovich factors, the angle is also approximate. The reason for this is that the matrix W^* needs to be calculated both for the accurate direction angle and the accurate Zeldovich factor. The challenge in the Stauffer description of two-component heterogeneous nucleation kinetics is posed by the numerical calculation of the matrix W^* involving solution of highly nonlinear (and sometimes numerically cumbersome, see end of Appendix A) Eq. (A1) described in Appendix A, from which the bulk mole fraction in the heterogeneous cluster with known total numbers of molecules can be solved. The approximations described in Eqs. (16), (20), (19), and (21) make it possible to avoid the calculation of the second derivatives of the formation energy.

C. Nucleation probability

In the case of heterogeneous nucleation it is often more practical to use the concept nucleation probability, instead of the nucleation rate, to quantify the process. In heterogeneous nucleation the amount of nucleated clusters (and thus the nucleation rate) is dependent on the amount of the pre-existing particles that act as CN. The nucleation probability indicates the fraction of the pre-existing particles that have become active as CN. The nucleation probability P in a set time period t is defined as (see, for example, Ref. 27),

$$P = 1 - \exp(-J \cdot 4\pi R_{CN}^2 \cdot t), \tag{27}$$

where the surface area of the CN is $4\pi R_{CN}^2$. For the nucleation time t we have used the value 10^{-3} s following the experiments we compare our model to. The values of the modeled onset activities for a chosen threshold nucleation probability P are not very strongly dependent on the selection of t.[28]

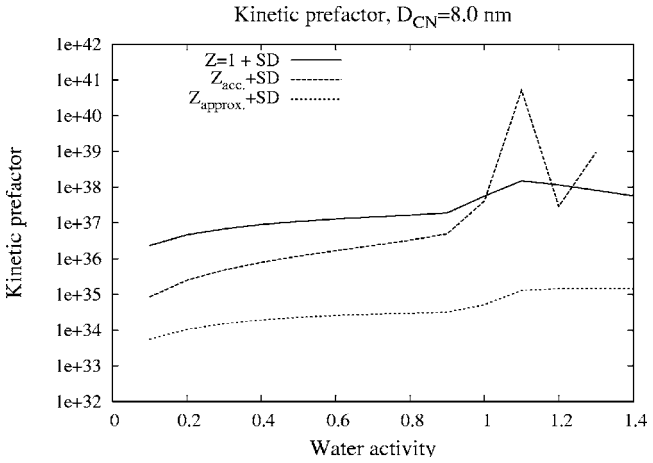

FIG. 2. The kinetic prefactor (for conditions at which nucleation probability $P>0.5$) for two-component nucleation with three models for condensation nuclei diameter of 8 nm. The temperature is $T=285$ K.

III. WATER-*n*-PROPANOL SYSTEM

A. Comparison with experiments: Setup and system properties

We tested the models by comparing them to three experiments conducted for water-*n*-propanol mixture nucleating on oxidized Ag particles with the average diameter of 8 nm.[28] The experiments were done using an expansion chamber, where an equilibrium vapor was produced with a spray-evaporation method from a liquid two-component mixture with constant propanol liquid mass fraction, after which the gas was supersaturated by expansion and consequent cooling[28] to nucleation temperature of $T=285$ K, which is the temperature used also in the model runs. The experiments were done for several propanol liquid mass fractions, but we chose three cases for the comparison with the models (mass fractions $X_l=0.653$, 0.763, and 0.926).

The same experimental data have been compared to earlier modeling results.[28] We used the thermodynamic data given in Ref. 29, and described in Appendix C, and the microscopic contact angle $\theta=35.82(1-x)/(1+61.62x)$ from Ref. 28. We applied the same data to derive the desorption and surface diffusion energies required for growth rates according to the surface diffusion. The only first-order guess made was the jumping distance of the molecule for *n*-propanol: there are no data available for *n*-propanol so we used the CO_2 value[10] since both molecules are nonpolar.

B. Sensitivity analysis of the kinetic prefactor

In this work we use the surface diffusion approach with three different versions of the Zeldovich factor: Table I describes them as $Z_{acc.}$+SD, $Z_{approx.}$+SD, and $Z=1$+SD. The difference in nucleation rates between the surface diffusion and the direct vapor deposition approaches 10^5-10^7,[26] which, however, does not affect significantly the prediction of nucleation onset,[23] since the onset is mainly controlled by the exponential part of the nucleation rate. Figure 2 shows

Downloaded 19 Dec 2007 to 128.214.182.209. Redistribution subject to AIP license or copyright; see http://jcp.aip.org/jcp/copyright.jsp

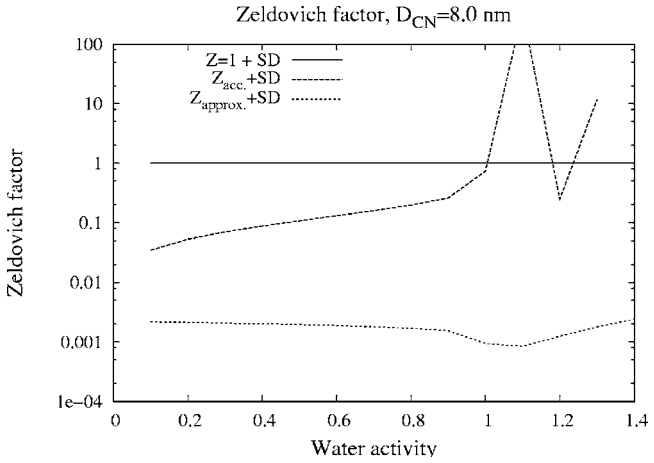

FIG. 3. The Zeldovich factor (nucleation probability $P>0.5$) for two-component nucleation with three models for condensation nuclei diameter of 8 nm. The temperature is $T=285$ K.

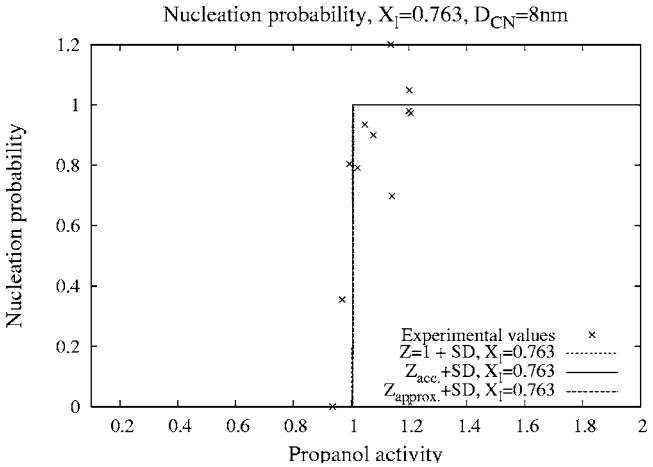

FIG. 5. Nucleation probability as a function of propanol activity with propanol liquid mass fraction of 0.763. The temperature is $T=285$ K and the diameter of the pre-existing particles $D_{CN}=8$ nm. Also plotted as crosses are the experimental data values for the specific propanol mass fraction.

the kinetic prefactors and Fig. 3 shows the Zeldovich factors for the three variants of the model for conditions at which $P=0.5$ as functions of water activity. The difference in the kinetic prefactor between the models originates mainly from the difference in the Zeldovich factors. The approximate growth angle Y plays a minor role. The Zeldovich factors, and thus the kinetic prefactors, differ 1–5 orders of magnitude, but this does not affect the prediction of the onset conditions as will be shown by the next four figures. The strange behavior of the kinetic prefactor in Fig. 2 and the Zeldovich factor in Fig. 3 at water activities 1–1.3 is due to numerical behavior of the Stauffer model with high water activities. The peak of the Zeldovich factor occurs where the physically relevant root of Eq. (A1) switches from one branch to another (see end of Appendix A).

C. Water-*n*-propanol: Results

For the monodisperse CN the probability plots (Figs. 4–6) are step functions, where the nucleation probability goes directly from zero to one. The case would not be the same for a wide CN size distribution, when the values of J for different CN sizes can vary significantly affecting the value of P which is integrated over the CN sizes. In the theoretical work we have used only monodisperse CN distribution. The particle size distribution was not completely monodisperse in the experiments,[28] which can be seen as a less steep behavior of the experimental data points.

The approximate treatment of the Zeldovich factor and the growth angle do not affect nucleation probabilities significantly. In all models the nucleation rate has a steplike jump from practically zero to a high value (and the nucleation probability jumps to the value of 1), and the jump occurs at the same activity values. Note that the experimental data points sometimes exceed the value of $P=1$, which is seen also in the original Ref. 28; this can be caused by the experimental setup, homogeneous nucleation in the chamber or approximations in the data analysis.

The activity plot (Fig. 7) shows the modeled onset activities (nucleation probability equals or exceeds 0.5) for three different condensation nuclei diameters and the experi-

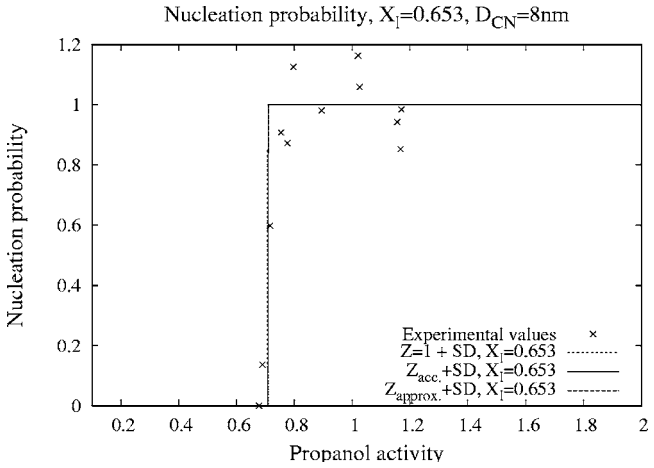

FIG. 4. Nucleation probability as a function of propanol activity with propanol liquid mass fraction of 0.653. The temperature is $T=285$ K and the diameter of the pre-existing particles $D_{CN}=8$ nm. Also plotted as crosses are the experimental data values for the specific propanol mass fraction.

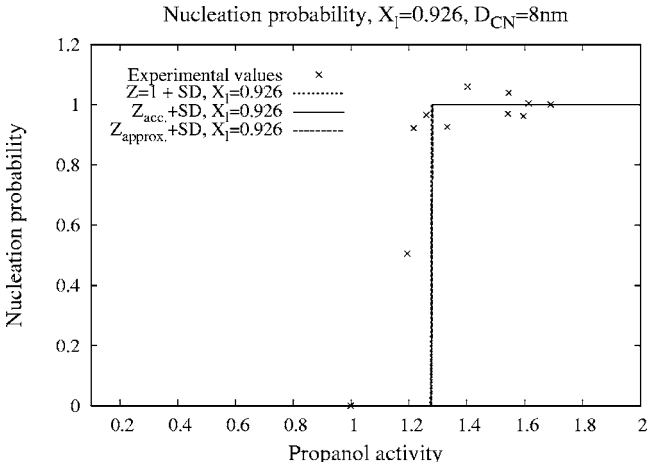

FIG. 6. Nucleation probability as a function of propanol activity with propanol liquid mass fraction of 0.926. The temperature is $T=285$ K and the diameter of the pre-existing particles $D_{CN}=8$ nm. Also plotted as crosses are the experimental data values for the specific propanol mass fraction.

Downloaded 19 Dec 2007 to 128.214.182.209. Redistribution subject to AIP license or copyright; see http://jcp.aip.org/jcp/copyright.jsp

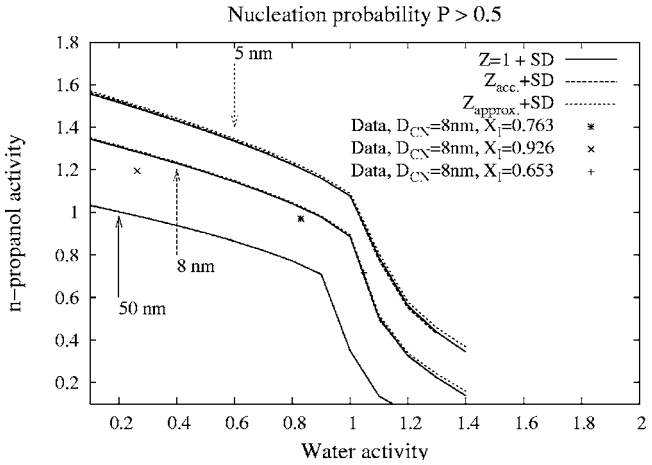

FIG. 7. The modeled onset activities (nucleation probability $P>0.5$) for two-component nucleation with three models for condensation nuclei diameters of 5, 8, and 50 nm. The temperature is $T=285$ K. The three points marked in the plot show the experimental data from measurements for approximately 8 nm diameter pre-existing particles and three *n*-propanol liquid mass fractions.

mental data for three *n*-propanol mass fractions. With larger CN the required activities for the onset of heterogeneous nucleation are lower. Figure 7 also shows that the classical nucleation theory reproduces well the shape of the curve and the correct magnitude of the experimental onset activities, but fails to quantitatively match the experiments. The activity plot also shows that the simplified models follow very well the curve of the Stauffer model, which indicates that the approximations made in the simplified models do not affect significantly the prediction of nucleation onset.

IV. THE MARTIAN WATER-CARBON DIOXIDE SYSTEM

A. System properties

The properties of the Martian two-component water-carbon dioxide system are not well known and in this work we are only interested in testing the possibilities for nucleation onset for this system. The one-component heterogeneous nucleation of both of these substances has been studied previously.[23] We have also tested the homogeneous nucleation of the components separately,[23] and based on the results we have neglected homogeneous two-component nucleation as unlikely to happen due to extremely high supersaturations required.

The parameters for the simulations are listed in Table II. The values for the adsorption and surface diffusion energies listed in Table II are taken to be the latent heat and one tenth of the latent heat, respectively, as in Ref. 30 and 31. The contact parameter of the mixture is calculated as $m_{\mathrm{mix}}=xm_1+(1-x)m_2$, where m_1 and m_2 are the contact parameters of the pure substances CO_2 and H_2O, respectively, and x is the mole fraction of component 1 (CO_2). As a first approximation, we have calculated the thermodynamic data (surface energy, ice density) for the mixture assuming ideal mixing. For ideal mixture, the solid (in this case the bulk phase corresponding to the clusters is solid) phase activities are equal to the mole fractions of the respective species. For testing the behavior of the system, we made model simulations also

TABLE II. Parameters for the Martian heterogeneous nucleation. The two rightmost columns present the value used and/or the reference for the used value.

Parameter	Symbol	CO_2	H_2O
Contact parameter	m	0.952 Ref. 40	0.97 Ref. 10
Energy of adsorption (J molecule^{-1})	ΔF_{des}	$3.25\cdot10^{-20}$ Ref. 30	$2.9\cdot10^{-20}$ Ref. 31
Energy of surface diffusion (J molecule^{-1})	ΔF_{sd}	$3.25\cdot10^{-21}$ Ref. 31	$2.9\cdot10^{-21}$ Ref. 31
Saturation vapor pressure (Pa)	p_{sat}	Ref. 33	Ref. 34 See Appendix B
Surface energy (J m^{-2})	σ	0.080 Ref. 10	0.106 Ref. 26
Ice density (kg m^{-3})	ρ_{ice}	1600.0, Ref. 10	Ref. 26
Molecular heat capacity (J K^{-1})	c_v	6.166e-23 calculated	4.66e-23 calculated
Vibrational frequency of the molecule (s^{-1})	ν	$2.9\cdot10^{12}$ Ref. 41	$1.0\cdot10^{13}$ Ref. 26
Jumping distance of the molecule (m)	d	$4.0\cdot10^{-10}$ Ref. 10	$3.2\cdot10^{-10}$ Ref. 26

using the activity coefficients of water-*n*-propanol system for the water-carbon dioxide system, since no data for the latter is available. As both CO_2 and *n*-propanol are nonpolar molecules, the activities of the water-*n*-propanol system are thought to mimic the real behavior of the H_2O-CO_2 system.

We made model runs for different temperatures with a CN radius of 1 μm, which is close to the average dust radius near the Martian surface. The temperature range of 140–285 K was chosen as an average range for the Martian near-surface temperatures. The effect of the CN radius was not specifically tested here, but generally for CN as large as 1 μm nucleation is easier than for smaller particles. However, nucleation is not infinitely facilitated by increasing the CN size, but levels off at some point. In our one-component nucleation studies[23] our tests showed that the decrease in nucleation rates is significant only for CN radii smaller than 100 nm, and for bigger CN the nucleation rates stay fairly constant. Thus, the effect of a wider CN distribution would be to decrease the integrated nucleation rate due to the contribution of the smaller particles, as the larger seed particles do not enhance the rate significantly.

B. The nonisothermal coefficient

In previous studies of CO_2 cloud formation in the Martian atmosphere a correction for latent heat effects in nucleation happening in a near-pure vapor has been used.[10,23] The nonisothermal correction has been derived for homogeneous nucleation where the effect is significant, but in heterogeneous nucleation the CN functions as a heat bath that thermalizes the cluster efficiently and a correction term is thus

Downloaded 19 Dec 2007 to 128.214.182.209. Redistribution subject to AIP license or copyright; see http://jcp.aip.org/jcp/copyright.jsp

not needed. Only in cases where the CN are smaller than the nucleating cluster, a nonisothermal correction may be needed also in heterogeneous nucleation and the effect may be significant also in ion-induced nucleation. The theoretical approach is anyhow revised here for our case of two-component nucleation, since we have performed our model runs both with and without the nonisothermal correction to be comparable with previous studies. The difference between the results for nucleation onset with and without the correction is insignificant: the onset activities differ only by $10^{-3}-10^{-2}$. The results of the following figures are calculated without a nonisothermal correction.

The nonisothermal coefficient $f_{\delta T}$, which is important in nucleation occurring in near-pure vapor without an excess of thermalizing inert carrier gas, is calculated using the formulation of Ref. 32, as was also done in Ref. 23,

$$f_{\delta T} = \frac{b^2}{b^2 + q^2}, \tag{28}$$

where q describes the energy acquired to the cluster in adhering of monomers of the nucleating gas, and b the energy lost in collisions of gas molecules with the cluster. b is of the form

$$b = (c_{v,i} + 0.5k)kT^2 + \frac{\beta_c}{\beta_i}(c_{v,c} + 0.5k)kT^2, \tag{29}$$

where $c_{v,i}$ is the molecular specific heat of the nucleating gas and $c_{v,c}$ that of the inert carrier gas. The impingement frequencies of the gases, β_c for the inert carrier gas and β_i for the nucleating gas, are calculated with the formula $\beta_{c/i} = p_{c/i}/\sqrt{2\pi m_{\text{molec.}}kT}$. $m_{\text{molec.}}$ is the molecular mass of the gas, which is calculated for the carrier gas as the weighed average of the gases (N_2, Ar, O_2). The partial pressure p_c is that of the carrier gas, p_i that of the nucleating gas. q in Eq. (28) can be written in the following form:

$$q = h - kT/2 - \sigma\frac{\partial A(n)}{\partial n}$$

where $A(n)$ is the cluster surface area as a function of the number of molecules in the cluster and h is the latent heat per molecule.

As an approximate extension to the two-component system, the partial pressure of the nucleating vapor p_i is calculated as the sum of the partial pressures of H_2O and CO_2, and the number of molecules in the critical cluster, needed to calculate the surface area of the cluster, is taken to be the sum of the core numbers of the two substances. These simplifications do not significantly affect the magnitude of the nonisothermal coefficient.

For calculating the partial pressure of the inert gas we use two approaches. In the onset study (Fig. 8) where the activities were allowed to change freely, the partial pressure of the inert gas (p_c, consisting mostly of nitrogen and argon) is calculated from the ratio of the inert gas and CO_2 in Mars (4.46%/95.32%), which should stay fairly constant. In the comparison study [Figs. 9(a) and 9(b)] the total pressure, H_2O pressure, and CO_2 pressure are fixed. Then the total pressure is the sum of all the partial pressures $p_{\text{atm}} = p_{H_2O} + p_{CO_2} + p_c$, and thus p_c can be calculated as $p_c = p_{\text{atm}} - (p_{H_2O} + p_{CO_2})$. The difference in these two ways of calculating the inert gas partial pressure is indistinguishable in our results.

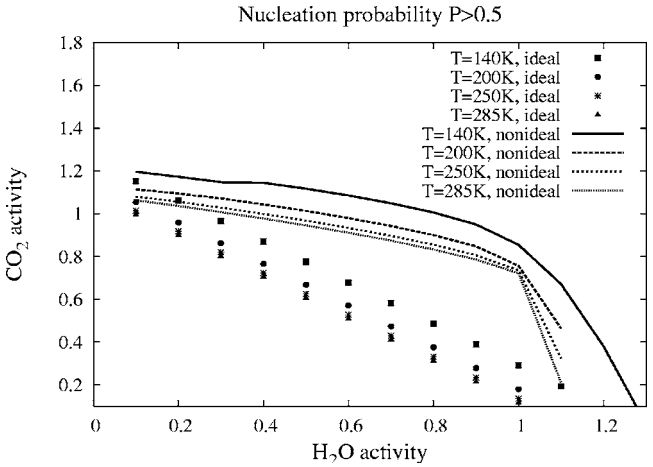

FIG. 8. An activity plot for H_2O-CO_2 system at temperatures 140–285 K and with condensation nuclei radius of 1 μm. The model used is accurate Zeldovich factor with surface diffusion approach, $Z_{\text{acc.}}$+SD.

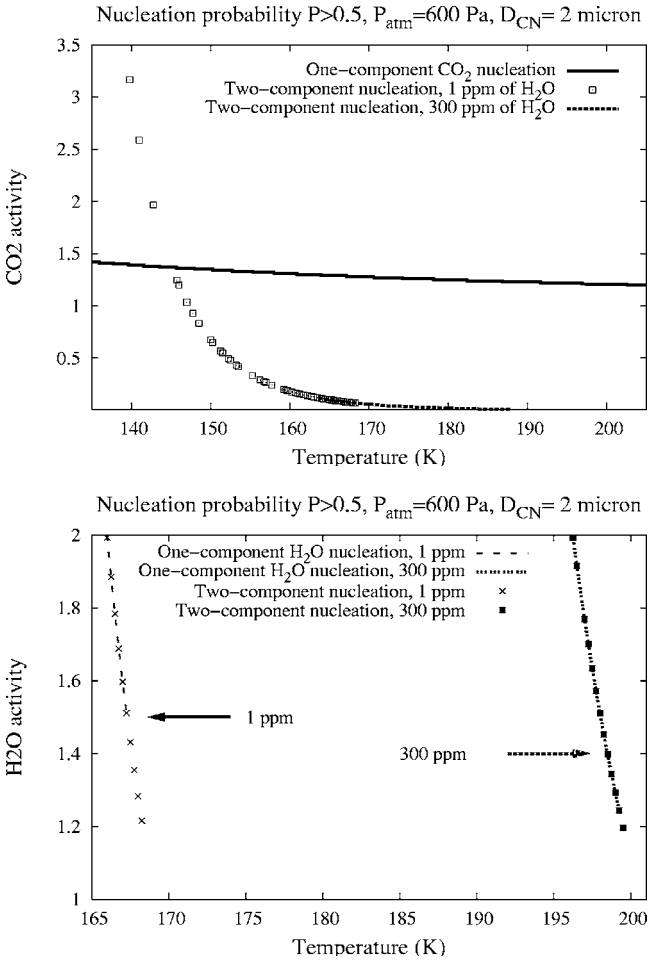

FIG. 9. The nucleation probability $P>0.5$ as a function of temperature and activity for atmospheric pressure of 600 Pa and condensation nuclei radius of 1 μm, (a) CO_2 and (b) H_2O. The amount of CO_2 is 95.32% and of H_2O 1 and 300 ppm. The model used is accurate Zeldovich factor with surface diffusion approach, $Z_{\text{acc.}}$+SD.

Downloaded 19 Dec 2007 to 128.214.182.209. Redistribution subject to AIP license or copyright; see http://jcp.aip.org/jcp/copyright.jsp

C. Water-CO_2: Results

For all the Martian studies we used the accurate Zeldovich factor [Eq. (18)] and growth angle [Eq. (15)] with the surface diffusion approach, $Z_{acc.}+SD$, in terms of Table I. The results presented here are calculated without the nonisothermal correction. The model predicts nucleation at all temperatures between 140 and 285 K, as can be seen from Fig. 8. The plot shows the ideal mixture assumption as a linear dependence between the activities. As we can see from Fig. 8, the nonideal mixture requires higher activities to nucleate, since for aqueous mixtures of nonpolar molecules nucleation does not happen as easily as for ideal mixtures.

As mentioned in Sec. IV B, even though the CN is an effective heat bath in heterogeneous nucleation, a correction for nonisothermal nucleation has been used in previous heterogeneous nucleation studies for CO_2 on Mars.[10,23] We have performed our calculations for Martian nucleation with and without the nonisothermal correction, and as can be expected, the difference in critical activities (nucleation onset) is insignificant $(10^{-3}-10^{-2})$, since the value of $f_{\delta T}$ is only of the order of 10^{-2}, and it affects the prefactor of nucleation rate equation, not the dominant exponential term. The nonisothermal coefficient was 0.02–0.03 for the range where the molecular numbers of both substances in the critical cluster were greater than one. This is in the same range as was acquired for one-component CO_2 nucleation in Ref. 23. The results here are presented without the nonisothermal correction.

We determined the critical activities corresponding to nucleation probability of $P>0.5$ for two-component nucleation of H_2O and CO_2 and for one-component nucleation of both substances. The amount of CO_2 was fixed to the present Martian value of 95.32%, and several values of water concentration (1–300 ppm) were tested. This means that the CO_2 and H_2O activities changed only with the changing temperature, which was chosen as the abscissa of Figs. 9(a) and 9(b). The atmospheric pressure is 600 Pa in this plot and the ideal mixture assumption was used. The ideal mixture assumption gives the lower limit of critical activities required, as seen from Fig. 8. Figures 9(a) and 9(b) show that the CO_2 concentration is not the limiting factor for the initiation of two-component nucleation, but the water amount is. Also the curves of critical water activity for two-component nucleation and the curve for one-component water nucleation exactly overlap for most of the temperature region where nucleation occurs. The points depicting two-component nucleation show that the onset of two-component nucleation happens at slightly lower activities than the onset of one-component nucleation, especially in the case of 1 ppm of water.

We looked at the numbers of molecules in the critical cluster in the cases where two-component nucleation happens in lower activities than one-component nucleation and noticed that the cluster is mainly composed of water molecules [Figs. 10(a) and 10(b)]. In some cases, like the 1 ppm case [Fig. 10(a)], the number of CO_2 molecules stays fairly large (tens of molecules) in a wide range of temperatures (about 1 deg), but in the 300 ppm case [Fig. 10(b)] the number of CO_2 molecules is at most 2–3, and it drops very quickly to less than one with decreasing temperature (which implies one-component water nucleation). So theoretically at the onset of water nucleation on Mars it seems that two-component nucleation might have a role in facilitating the process, but the number of CO_2 molecules in the critical clusters is very small, and particle formation process is very close to pure water nucleation. The smaller the water amount in the vapor phase is, the more CO_2 molecules there are in the critical cluster.

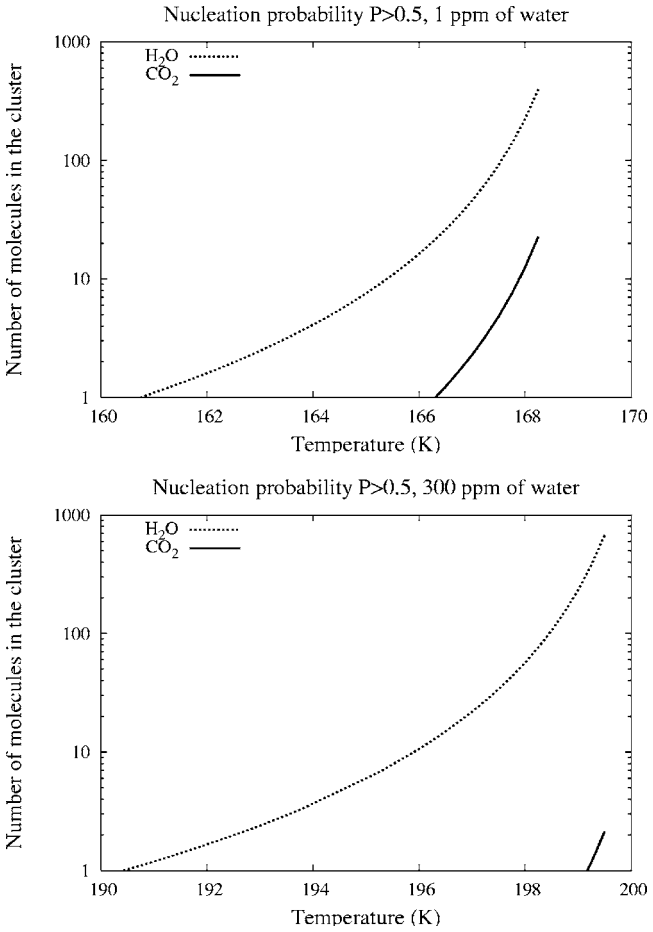

FIG. 10. The numbers of molecules in the critical clusters for the cases in Fig. 9(b). The amount of H_2O is (a) 1 and (b) 300 ppm. The model used is accurate Zeldovich factor with surface diffusion approach, $Z_{acc.}+SD$.

For CO_2 the case is simple: at around 145 K in Fig. 9(a) it is clearly seen that the critical CO_2 activity curve of two-component nucleation goes above the one-component curve, which tells that below that temperature nucleation is pure CO_2 nucleation, since the critical activity required is always lower than the one required for two-component nucleation.

Thus according to our results we cannot completely rule out the possibility of two-component nucleation of the CO_2-H_2O mixture, possibly at the very first stages of one-component water nucleation, and especially for small water vapor amounts. This result is naturally dependent on the assumptions made for the system properties (especially the ideal mixture assumption) and validating the results will have to wait until there are data for the real thermodynamic properties of the system. We can conclude that in the present

Downloaded 19 Dec 2007 to 128.214.182.209. Redistribution subject to AIP license or copyright; see http://jcp.aip.org/jcp/copyright.jsp

Martian atmosphere according to observations of cloud properties and previous modeling, ice crystals do form dominantly for one component at a time, as also described in our earlier paper[23] and several other authors.[8–16] Two-component nucleation is still an open question and our work in this paper calls for more research on the interesting topic.

V. DISCUSSION AND CONCLUSIONS

Embracing the opportunity of increased computer power we developed a two-component heterogeneous nucleation model using the exact Stauffer steady-state kinetics.[19] We also used two models with simplified kinetics for comparison. The comparison between the models and water-*n*-propanol experiments showed that also the simpler models are good tools for describing two-component nucleation: the nucleation onset is predicted at nearly the same critical activities in the models.

The Martian aerosol dynamics is an interesting topic, since the Martian atmosphere is so different compared to its terrestrial counterpart. The vapors involved in aerosol and cloud formation differ, as do their roles in the process, like the condensation in near-pure vapor for CO_2. Cloud formation must be frequent in the Martian atmosphere since clouds are constantly observed. On Mars the major constituent of the atmosphere, CO_2, is involved in the cloud formation processes and calls for re-evaluation of the theories formulated for trace gases nucleating and condensing in the atmosphere of the Earth. For example, in condensation in a near-pure vapor the latent heat release and changes in the composition of the gas near the particle must be considered. So far only one-component processes have been looked into, but as on Earth, it can be speculated that multicomponent nucleation and condensation may have a role in cloud formation in the Martian atmosphere.

The lack of data for the thermodynamic properties of the H_2O-CO_2 mixture is the by far most important difficulty in modeling two-component nucleation for Mars. In this study we tested two possibilities: an ideal mixture and a nonideal mixture with the mixing properties of water-*n*-propanol mixture. The latter resembles the behavior of the H_2O-CO_2 mixture since both the *n*-propanol and CO_2 molecules are nonpolar, which implies the mixture to be less favorable to nucleation than the ideal one. We also discussed and tested the previously used nonisothermal factor in heterogeneous CO_2 nucleation: the correction is unnecessary, but the effect it has is negligible in the studies we have performed.

Our studies here show that two-component nucleation is theoretically possible in the Martian atmosphere and seemingly coupled to the onset of one-component nucleation of water. The initiation of water nucleation (especially with low water amount in the vapor phase) involves critical clusters containing CO_2 molecules mixed with a larger amount of H_2O molecules. The numbers of CO_2 molecules in the cluster are the higher the lower the water vapor concentration in the vapor phase is. The one-component water nucleation model supports the result of the two-component model, since the calculated critical activities mostly overlap.

We can assume that most probably the aerosol dynamical studies and cloud models for the Martian atmosphere can focus on one component at a time, since at the moment we have only highly theoretical results on the possibilities of two-component nucleation on Mars, and observations show clouds composed of either water or carbon dioxide ice. Remote sensing observations, however, cannot observe particle formation, and thus studies of the composition of the formed critical clusters in the conditions of our model runs would be very important for validating our results and giving more insight into Martian cloud formation. Thus in the future hopefully there will be more data on the properties of CO_2 and H_2O and their mixture to study accurately the onset of two-component nucleation. Also testing the nucleation model coupled with an atmospheric model (for example in the polar night) would help constraining better the processes of cloud formation on Mars.

ACKNOWLEDGMENTS

This work was supported by the Academy of Finland, the Kordelin Foundation, and the Graduate School of Astronomy and Space Physics.

APPENDIX A: FORMATION FREE ENERGY FOR A GENERAL CLUSTER

To calculate the second derivatives needed for matrix W^*, we need to calculate the formation free energy of a noncritical cluster with known total number of molecules $n_{1,\mathrm{tot}}^{\mathrm{het}}$ and $n_{2,\mathrm{tot}}^{\mathrm{het}}$. First, the mole fraction in the core of the cluster needs to be solved from equation

$$x\left[n_{1,\mathrm{tot}}^{\mathrm{het}} - \sum_s n_{1,s}^{\mathrm{het}}(x,r^*)\right] - (1-x)\left[n_{2,\mathrm{tot}}^{\mathrm{het}} - \sum_s n_{2,s}^{\mathrm{het}}(x,r^*)\right] = 0, \tag{A1}$$

which is valid since $x = n_{2,l}^{\mathrm{het}}/(n_{1,l}^{\mathrm{het}} + n_{2,l}^{\mathrm{het}})$ and $n_{i,\mathrm{tot}}^{\mathrm{het}} = n_{i,l}^{\mathrm{het}} + \Sigma_s n_{i,s}^{\mathrm{het}}$. For Eq. (A1) the surface excess numbers are given by Eqs. (9). The radius of the cluster needed in Eqs. (9) is solved from equation

$$V_{\mathrm{het}} = n_{1,\mathrm{tot}}^{\mathrm{het}} v_1(x) + n_{2,\mathrm{tot}}^{\mathrm{het}} v_2(x) = f_n(r)\tfrac{4}{3}\pi r^3. \tag{A2}$$

Equation (A2) follows from $V_{\mathrm{het}} = \Sigma_i n_{i,l}^{het} v_i$ and the equimolar surface conditions

$$\sum_i n_{i,s}^{\mathrm{het}} v_i = 0. \tag{A3}$$

The formation energy of a cluster is then given by[22,25]

$$\Delta G_{\mathrm{het}} = 2\pi r^2 \sigma_{g,l}\left(1 + \frac{1 - Xm}{g}\right) - 2\pi R_{\mathrm{CN}}^2(\sigma_{l,\mathrm{sol}} - \sigma_{g,\mathrm{sol}}) \times \left(1 + \frac{X - m}{g}\right) + \sum_i \Delta\mu_i n_{i,l}^{\mathrm{het}} + \sum_{i,s} (\mu_{i,s} - \mu_{i,g}) n_{i,s}^{\mathrm{het}}, \tag{A4}$$

where $\mu_{i,s}$ is the chemical potential of the surface s, and $\mu_{i,g}$ is the chemical potential in the gas phase.

Downloaded 19 Dec 2007 to 128.214.182.209. Redistribution subject to AIP license or copyright; see http://jcp.aip.org/jcp/copyright.jsp

As in deriving Eqs. (9) (Ref. 24) we assume that even in a noncritical cluster the chemical potentials in the surface phases are the same as the chemical potentials in the liquid

$$\mu_{i,s} = \mu_{i,l} \tag{A5}$$

and use the result[25]

$$\mu_{i,l} - \mu_{i,g} = \Delta\mu_i + \frac{2\sigma_{g,l}v_i}{r} \tag{A6}$$

to get

$$\Delta G_{\text{het}} = 2\pi r^2\sigma_{g,l}\left(1 + \frac{1 - Xm}{g}\right) - 2\pi R_{\text{CN}}^2(\sigma_{l,\text{sol}} - \sigma_{g,\text{sol}}) \times\left(1 + \frac{X - m}{g}\right) + \sum_{i,s}\Delta\mu_i(n_{i,l}^{\text{het}} + n_{i,s}^{\text{het}}) + \frac{2\sigma_{g,l}}{r}\left(\sum_{i,s} v_i n_{i,s}^{\text{het}}\right). \tag{A7}$$

Using the equimolar surface conditions (A3) and the Young's equation [Eq. (6)] for the surface tensions, we finally obtain

$$\Delta G_{\text{het}} = 2\pi r^2\sigma_{g,l}\left(1 + \frac{1 - Xm}{g}\right) - 2\pi R_{\text{CN}}^2 m\sigma_{g,l} \times\left(1 + \frac{X - m}{g}\right) + \sum_{i}\Delta\mu_i n_{i,\text{tot}}^{\text{het}}. \tag{A8}$$

To obtain the second derivatives the differentiations are performed numerically. In the activity region where the surface excess contributions are large (and the applicability of classical theory thus suspect) Eq. (A1) can have three roots, instead of a single root, for $0 < x < 1$. In these cases we have checked which of the branches gives the correct critical cluster core composition when the total numbers of molecules in the critical cluster are inserted into Eq. (A1). We then used the same (first, second, or third from the left) branch for the cases slightly off the critical cluster needed for the second derivatives.

APPENDIX B: SATURATION VAPOR PRESSURES OF CO_2 AND H_2O

The saturation vapor pressures for the Martian substances used in the models are the following. For CO_2 the saturation vapor pressure curve can be expressed as in Ref. 33

$$\log_{10}P_{\text{sat,CO}_2} = 3.128082 - \frac{867.2124}{T} + 18.65612\cdot 10^{-3}T - 72.48820\cdot 10^{-6}T^2 + 93\cdot 10^{-9}T^3 \tag{B1}$$

for $T > 216.56$ K and

$$\log_{10}P_{\text{sat,CO}_2} = 6.760956 - \frac{1284.07}{T - 4.718} + 1.256\cdot 10^{-4}(T - 143.15) \tag{B2}$$

for $T < 216.56$ K. These equations give P in atmospheres (1 atm = 101 325.0 Pa) and the temperature is given in Kelvin degrees.

For H_2O the equation given in Ref. 34 has been modified here so that the temperature can be put in directly as Kelvin degrees

$$P_{\text{sat,H}_2\text{O}} = 611.15\cdot\exp\left(22.542\frac{T - 273.16}{T + 0.32}\right). \tag{B3}$$

This equation gives P in pascals.

APPENDIX C: THERMODYNAMIC DATA FOR THE WATER-*n*-PROPANOL SYSTEM

This appendix gives the thermodynamic data used in the model runs for the system water-*n*-propanol. The saturation vapor pressures used are described by the following equations:[35,36]

$$p_{\text{H}_2\text{O}} = \exp\left(77.34491296 - \frac{7235.424651}{T} - 8.2\ln T + 5.7113\cdot 10^{-3}T\right), \tag{C1}$$

$$p_{\text{C}_3\text{H}_8\text{O}} = \exp\left(89.5883 - \frac{8559.6064}{T} - 9.29\ln T\right) \tag{C2}$$

for water and *n*-propanol, respectively. The equations give the pressure in pascals and the temperature is in Kelvin degrees.

The density of the water-*n*-propanol mixture is given by[37]

$$\rho_{\text{H}_2\text{O}+\text{C}_3\text{H}_8\text{O}} = X_m\rho_p + (1 - X_m)\rho_w, \tag{C3}$$

where X_m is the mass fraction of *n*-propanol in the mixture. ρ_p is the density of *n*-propanol, given by the following equation:

$$\rho_p = 1047.94 - 0.835978T, \tag{C4}$$

and ρ_{w} is the density of water, given by equations

$$\rho_w = \frac{w_1}{w_2}, \tag{C5}$$

$$w_1 = 999.83952 + 16.945176T_c - 7.9870401\cdot 10^{-3}T_c^2 - 46.170461\cdot 10^{-6}T_c^3 + 105.56302\cdot 10^{-9}T_c^4 - 280.54253\cdot 10^{-12}T_c^5,$$

$$w_2 = 1 + 16.87985\cdot 10^{-3}T_c,$$

where $T_c = T - 273.15$ K. All densities are expressed in kg m^{-3} and temperatures in Kelvin degrees.

The surface tension for the liquid mixture is[38]

Downloaded 19 Dec 2007 to 128.214.182.209. Redistribution subject to AIP license or copyright; see http://jcp.aip.org/jcp/copyright.jsp

$$\sigma_{H_2O+C_3H_8O} = 0.001 \exp(\sigma_1 + \sigma_2 + \sigma_3 + \sigma_4 + \sigma_5), \quad \text{(C6)}$$

where

$$\sigma_1 = 4.811191 - 1.951091 \times 10^{-3}T, \quad \text{if } y \geq 0.006,$$

$$\sigma_1 = 4.859191 - 1.951091 \times 10^{-3}T - 8y, \quad \text{if } y < 0.006,$$

$$\sigma_2 = (5.723187 - 0.03852713T) \cdot y,$$

$$\sigma_3 = (-32.01079 + 0.1481755T) \cdot y^2,$$

$$\sigma_4 = (45.29557 - 0.1891045T) \cdot y^3,$$

$$\sigma_5 = (-19.68398 + 0.07811035T) \cdot y^4,$$

where $y = 7x/(1+6x)$ and x is the mole fraction of *n*-propanol in the mixture. The temperatures are in Kelvin degrees.

The activity coefficients for the mixture were calculated using the parametrization of Ref. 39.

[1] G. E. Hunt and P. B. James, Adv. Space Res. **5**, 93 (1985).
[2] G. H. Pettengill and P. G. Ford, Geophys. Res. Lett. **27**, 609 (2000).
[3] A. B. Ivanov and D. O. Muhleman, Icarus **154**, 190 (2001).
[4] L. K. Tamppari, R. W. Zurek, and D. A. Paige, J. Geophys. Res. **108**, 5073 (2003).
[5] F. Montmessin, J.-L. Bertaux, E. Quemerais *et al.*, Icarus **183**, 403 (2006).
[6] F. Montmessin, B. Gondet, T. Fouchet, P. Drossart, J.-P. Bibring, J.-L. Bertaux, and Y. Langevin, American Geophysical Union, Fall Meeting 2006, abstract P14A–03.
[7] F. Montmessin, B. Gondet, J.-P. Bibring, Y. Langevin, P. Drossart, F. Forget, and T. Fouchet, J. Geophys. Res. (to be published).
[8] D. V. Michelangeli, O. B. Toon, R. M. Haberle, and J. B. Pollack, Icarus **100**, 261 (1993).
[9] A. Colaprete, O. B. Toon, and J. A. Magalhaes, J. Geophys. Res. **104**, 9043 (1999).
[10] S. E. Wood, Ph.D. thesis, University of California, Los Angeles, 1999.
[11] A. Inada, Ph.D. thesis, Kobe University, Japan, 2002.
[12] A. Colaprete and O. B. Toon, J. Geophys. Res. **107**, 5051 (2002).
[13] A. Colaprete and O. B. Toon, J. Geophys. Res. **108**, 5025 (2003).
[14] G. Tobie, F. Forget, and F. Lott, Icarus **164**, 33 (2003).
[15] F. Montmessin, P. Rannou, and M. Cabane, J. Geophys. Res. **107**, 5037 (2002).
[16] M. I. Richardson, R. J. Wilson, and A. V. Rodin, J. Geophys. Res. **107**, 5064 (2002).
[17] J. Longhi, J. Geophys. Res. **111**, E06011 (2006).
[18] B. Schmitt, L. Mulato, and S. Doute, *Proceedings of the Third Mars Polar Science and Exploration Conference*, LPI Contributions (Lunar and Planetary Institute, Houston, TX, 2003).
[19] D. Stauffer, J. Aerosol Sci. **7**, 319 (1976).
[20] H. Trinkaus, Phys. Rev. B **27**, 7372 (1983).
[21] H. Reiss, J. Chem. Phys. **18**, 840 (1950).
[22] N. Fletcher, J. Chem. Phys. **29**, 572 (1958).
[23] A. Määttänen, H. Vehkamäki, A. Lauri, S. Merikallio, J. Kauhanen, H. Savijärvi, and M. Kulmala, J. Geophys. Res. **110**, E02002 (2005).
[24] M. Noppel, H. Vehkamäki, and M. Kulmala, J. Chem. Phys. **116**, 218 (2002).
[25] H. Vehkamäki, *Classical Nucleation Theory in Multicomponent Systems* (Springer, Berlin, 2006).
[26] H. R. Pruppacher and J. D. Klett, *Microphysics of Clouds and Precipitation* (Kluwer Academic, Norwell, MA, 1997).
[27] M. Lazaridis, M. Kulmala, and B. Z. Gorbunov, J. Aerosol Sci. **23**, 457 (1992).
[28] P. Wagner, D. Kaller, A. Vrtala, A. Lauri, M. Kulmala, and A. Laaksonen, Phys. Rev. E **67**, 021605 (2003).
[29] M. Kulmala, A. Lauri, H. Vehkamäki, A. Laaksonen, D. Petersen, and P. E. Wagner, J. Phys. Chem. B **105**, 11800 (2001).
[30] A. P. Zent and R. C. Quinn, J. Geophys. Res. **100**, 5341 (1995).
[31] J. Seki and H. Hasegawa, Astrophys. Space Sci. **94**, 177 (1983).
[32] J. Feder, K. C. Russell, J. Lothe, and G. M. Pound, Adv. Phys. **15**, 111 (1966).
[33] J. F. Kasting, Icarus **94**, 1 (1991).
[34] A. L. Buck, J. Appl. Meteorol. **20**, 1527 (1981).
[35] O. Preining, P. E. Wagner, F. G. Pohl, and W. Szymanski, *Heterogeneous Nucleation and Droplet Growth* (University of Vienna, Institute of Experimental Physics, Vienna, Austria, 1981).
[36] T. Schmeling and R. Strey, Ber. Bunsenges. Phys. Chem **87**, 871 (1983).
[37] G. S. Kell, J. Chem. Eng. Data **20**, 97 (1975).
[38] B. Y. Teitelbaum, T. A. Gortalova, and E. E. Siderova, Zh. Fiz. Khim. **25**, 911 (1951).
[39] Y. Viisanen, P. E. Wagner, and R. Strey, J. Chem. Phys. **108**, 4257 (1998).
[40] D. L. Glandorf, A. Colaprete, M. A. Tolbert, and O. B. Toon, Icarus **160**, 66 (2002).
[41] S. A. Sandford and L. J. Allamandola, Astrophys. J. **355**, 357 (1990).

Downloaded 19 Dec 2007 to 128.214.182.209. Redistribution subject to AIP license or copyright; see http://jcp.aip.org/jcp/copyright.jsp